

Majercsik, L., Gliozzi, A. and Munteanu, L., 2016. On the composites with negative stiffness inclusions. *Romanian Journal of Technical Sciences - Applied Mechanics*, 61(2), pp.161-175.

## ON THE COMPOSITES WITH NEGATIVE STIFFNESS INCLUSIONS

LUCIANA MAJERCSIK<sup>1</sup>, ANTONIO S. GLIOZZI<sup>2</sup>, LIGIA MUNTEANU<sup>3</sup>

*Abstract.* The paper discusses a composite consisted by the negative stiffness inclusion encapsulated by a polymer matrix. Negative stiffness inclusions exhibit an unusual behavior: when they are subjected to a mechanical load, after a certain force and during a certain displacement (still in the elastic region), the force decreases with displacement. In other words, the structure displays a negative stiffness (a negative slope) in a particular portion of its load-displacement curve. This property is usually unstable, but the inclusions of negative stiffness can be stabilized within a positive-stiffness material. The negative stiffness mechanism and incorporating into the matrix are defined in terms of the Eshelby's steps: 1) a FCC crystal cell belonging to the cubic system is subjected to a stress-free biaxial deformation in the [111] direction, becoming trigonal; 2) apply a surface biaxial traction to the trigonal crystal to be incorporated into the polymeric matrix, by assuring the continuity of displacements and normal stresses across the boundaries. The Young elastic modulus and damping capacity of this composite are discussed.

*Keywords:* composites, cellular materials, negative stiffness material, chess board structure, damping

### 1. INTRODUCTION

The concept of incorporating negative stiffness elements within mechanical systems was validated more than 40 years ago, but did not received consistent attention [1–3]. New recent metamaterial having implemented inclusions of negative stiffness have called the attention of researchers. An increase of several orders of magnitude of the damping ratio for the flexural waves propagating within a linear oscillator incorporating a negative stiffness element was demonstrated by Chronopoulos *et al.* [1]. The acoustic transmission in layered metamaterial including negative stiffness elements exhibits highly superior acoustic insulation performance close and above the acoustic coincidence range [2].

---

<sup>1</sup> Technical University of Civil Engineering, Bucharest

<sup>2</sup> Politecnico di Torino, DISAT – Dipartimento Scienza Applicata e Tecnologia

<sup>3</sup> Institute of Solid Mechanics of the Romanian Academy, Bucharest

The presence of inclusions of negative stiffness in composites, extremely high values of mechanical damping is achieved. Negative stiffness is of itself usually unstable but can be stabilized by incorporation in heterogeneous structures.

Negative stiffness is associated with buckling on a macroscopic scale or on an interatomic scale associated with phase transformations [4–8]. The unstable material models are essentially ill-posed according to classical definitions such as given by the Lax equivalence theorem [9].

For this reason, some authors show theoretically and experimentally, that composites with negative stiffness inclusions are characterized by a greater deformation in and near inclusions than the composite as a whole, and consequently exhibit interesting properties which exceed conventional bounds having higher stiffness and damping than that of either composites [10, 11]. A type of unstable material model is a material with negative elastic constants or moduli, which is often called strain-softening. A stress-strain curve with strain softening is shown in Fig. 1.

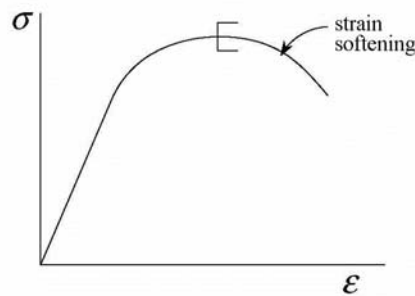


Fig. 1 — The material instability arises due to strain softening.

The reason that these negative stiffness inclusions are implemented in homogeneous matrices is that the final properties of the composite exhibit a good degree of stiffness and in addition, high energy absorbance property [1–3]. Nevertheless, there exists a natural limitation to the combination of the matrix and the inclusion material, meaning that homogenous materials with high stiffness, such as metals or ceramics, possess low damping, and vice versa. When composites are made by mixing materials with high and high loss materials, there occurs an inevitable tradeoff between the two properties, resulting in materials that present moderate stiffness and moderate damping. The negative stiffness inclusions are capable of controlling the deformation. The negative stiffness inclusions are excellent mechanisms for use in vibrational and acoustic damping [3].

In consequence, it is expected that the embedding of negative stiffness inclusions within a polymeric matrix will not only increase the stiffness of the polymer but will produce a composite material with superior damping capacity to that of any known natural material.

## 2. THE THEORY

Let assume that an FCC crystal cell belonging to the cubic system with three independent elastic constants, that is deformed in the  $[111]$  direction by an axis  $X$  parallel to  $OD$  (diagonal of the cube) and normal to  $ABC$  [11, 14]. The deformation can be analyzed by considering three sets of axes, all centered in  $O$ : a set of axes  $(x, y, z)$  parallel to three sides of the cube, an auxiliary set of axes  $(x', y', z')$  obtained from  $(x, y, z)$  with a  $45^\circ$  rotation around  $z \equiv z'$ , a third set of axes  $(X, Y, Z)$  obtained (Fig.2) from  $(x', y', z')$  with a rotation around  $y' \equiv Y$  of an angle  $\theta = \arcsin(1/\sqrt{3})$ . The transformation equations from  $(x, y, z)$  to  $(X, Y, Z)$  are given by

$$X = (x + y + z)/\sqrt{3}, \quad Y = (-x + y)/\sqrt{2}, \quad Z = (-x - y + 2z)/\sqrt{6}. \quad (1)$$

All allowed positions for atoms in an underformed FCC crystal (Fig. 3) may be specified by coordinates  $x, y, z$  which are integer or half-integer multiples of the lattice constant  $a$ , the only restriction being that  $x + y + z$  must be an integer multiplier of  $a$ .

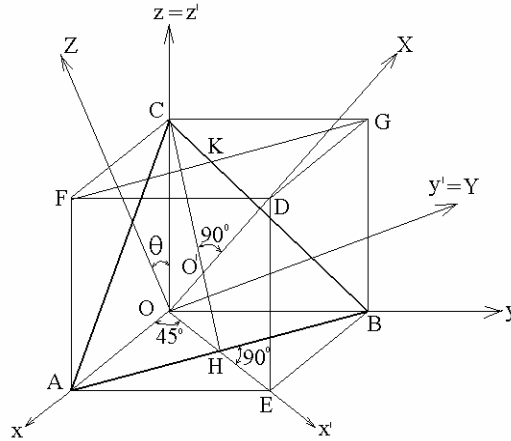


Fig. 2 – Representation of the sets of axes  $(x, y, z)$   $(x', y', z')$  and  $(X, Y, Z)$ .

The later is used to study the crystal in a biaxial deformed state.

Applying (1) we find that the corresponding coordinates in the  $(X, Y, Z)$  reference system are

$$X = la/\sqrt{3}, \quad Y = ma/\sqrt{8}, \quad Z = na/\sqrt{24}, \quad (2)$$

where  $l, m, n$  are integers, the only restrictions being that  $m$  and  $n$  must have the same parity.

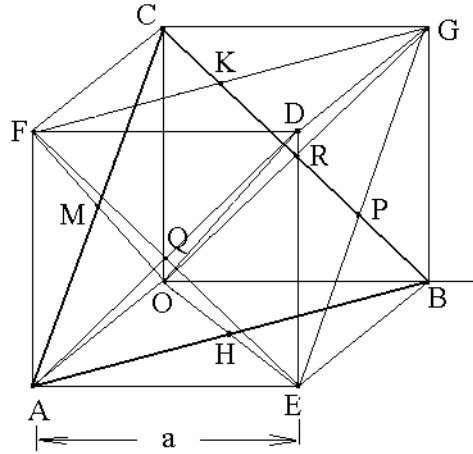


Fig. 3 – The FCC unit crystal cell.

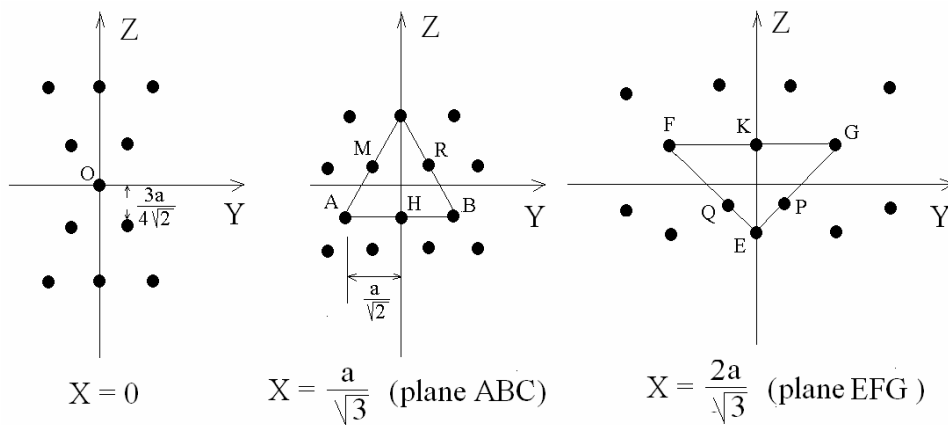


Fig. 4 – Lattice representation in the (X, Y, Z) reference system.

Figure 4 shows the lattice arrangement, as obtained from (2), for the plane ABC,  $X = a/\sqrt{3}$  and two neighboring planes  $X = 0$  and  $X = 2a/\sqrt{3}$ , except for the lattice point D, which lies in the plane  $X = 3a/\sqrt{3}$ . Using (2), the eight nearest neighbors to any atom (say the atom at O) are represented. Fig. 5 shows them schematically both in the  $(x, y, z)$  and  $(X, Y, Z)$  systems of axes. In the underformed crystal they are located at  $a/\sqrt{2}$ . A biaxial deformation in the [111] direction is described by

$$X_1 = X(1 + \epsilon'), \quad X_2 = Y(1 + \epsilon), \quad X_3 = Z(1 + \epsilon), \quad (3)$$

where  $X_i$  are the coordinates of the lattice positions in the initial deformed state, after the biaxial deformation, but before the infinitesimal deformation, and  $\varepsilon' = -2\varepsilon C_{1122} / C_{1111}$ .

The coordinates of the twelve nearest neighbors after the biaxial deformation are calculated from (3) in  $(x, y, z)$  system (Fig. 5a) and in  $(X, Y, Z)$  system (Fig. 5b). In Fig. 5b we see that  $a$  becomes  $a(1 + \varepsilon')$  and, in the planes themselves,  $a(1 + \varepsilon)$ . It then becomes straightforward, to calculate all the sums over the nearest neighbors and obtain explicit expressions for elastic constants. Although we may assume a priori that in the deformed state the crystal loses all its symmetries, becoming triclinic, it can be proved either by crystallographic arguments or directly through our calculations, that crystal retains trigonal symmetry (three planes of mirror symmetry). The trigonal crystal system is the only crystal system whose point groups have more than one lattice system associated with their space groups: the hexagonal (7 elastic constants) and rhombohedral lattices (9 elastic constants) both appear. Examples in nature of this kind of material are dolomite, quartz, beryl.

It can be easily shown that the transformation equations from  $(x, y, z)$  to  $(X, Y, Z)$  are

$$X = (x + y + z) / \sqrt{3}, \quad Y = (-x + y) / \sqrt{2}, \quad Z = (-x - y + 2z) / \sqrt{6}. \quad (4)$$

All allowed positions for atoms in the underformed FCC crystal may be specified by coordinates  $x, y, z$  which are integer or half-integer multiples of the lattice constant  $a$ , the only restriction being that  $x + y + z$  must be an integer multiplier of  $a$ . We find from (4) that the corresponding coordinates in the  $(X, Y, Z)$  reference system are

$$X = la / \sqrt{3}, \quad Y = ma / \sqrt{8}, \quad Z = na / \sqrt{24}, \quad (5)$$

where  $l, m, n$  are integers, the only restrictions being that  $m$  and  $n$  must have the same parity.

To calculate the elastic constants of the deformed FCC crystal, the Jankowski and Tsakalagos model material is adopted [12, 13]. According to this model the total crystal energy of metal may be written as

$$E = E_{es} + E_{fe} + E_{bs} + E_r, \quad (6)$$

where  $E_{es}$  represents the Madelung energy i.e. the electrostatic Coulomb energy of positive point charges in the uniform negative-charge background,  $E_{fe}$  is the free-electron energy, which depends on the crystal volume,  $E_{bs}$  is the band-structure energy and,  $E_r$  the Born-Mayer repulsive ion-core energy term. Jankowski and

Tsakalakos conclude that  $E_r$  is the predominant term for calculations of elastic constants. The energy term  $E_r$  can be expressed as

$$E_r = \frac{1}{2} \alpha \sum_R \exp(-\beta R), \quad (7)$$

where  $\alpha$ ,  $\beta$  are the repulsive energy parameter and respectively, the repulsive range parameter. The sum is extended to the nearest neighbors who are located at distances  $R^{(n)}$ . The second-order elastic constants (stiffness constants) are defined as

$$C_{ijkl} = \frac{\partial^2 \tilde{V}}{\partial \varepsilon_{ij} \partial \varepsilon_{kl}}, \quad \tilde{V} = \frac{E}{\Omega}, \quad (8)$$

where  $\tilde{V}$  is the potential energy of deformation per unit volume (or elastic potential),  $\Omega$  is the cell volume and  $\varepsilon_{ij}$  is the Lagrangian strain tensor. Starting with (6)–(8), the elastic constants are determined as [14]

$$\frac{\partial}{\partial \varepsilon_{ij}} = \frac{1}{2} (X_i \frac{\partial}{\partial x_j} + X_j \frac{\partial}{\partial x_i}), \quad (9)$$

where  $X_i$  are the Lagrangian coordinates corresponding to an initial state subjected to an initial finite deformation,  $x_i$  are the final Eulerian coordinates, differing from  $X_i$  by an infinitesimal deformation. The Lagrangian coordinates  $X_i$  are constants since they refer to a predefined initial state. From (6)–(8) it follows that

$$\begin{aligned} C_{ijkl} &= A_{ijkl} - B_{ijkl}, \quad A_{ijkl} = \sum_n f^{(n)} Y_{ijkl}^{(n)}, \\ B_{ijkl} &= \sum_n g^{(n)} Z_{ijkl}^{(n)} \quad f^{(n)} = f(R^{(n)}) = 4g^{(n)} \left( 1 + \frac{\beta R^{(n)}}{(R^{(n)})^2} \right), \\ g^{(n)} &= g(R^{(n)}) = \frac{K}{R^{(n)}} \exp(-\beta R^{(n)}), \quad K = \frac{\alpha \beta}{8\Omega}, \end{aligned}$$

where  $Y^{(n)}$ ,  $Z^{(n)}$  and  $R^{(n)}$  are calculated for the  $n$ -th nearest neighbor, as

$$\begin{aligned} Y_{ijkl} &= X_i X_j X_k X_l, \quad R = \sqrt{X_1^2 + X_2^2 + X_3^2}, \\ Z_{ijkl} &= X_i X_k \delta_{jl} + X_i X_l \delta_{jk} + X_j X_l \delta_{ik} + X_j X_k \delta_{il}. \end{aligned}$$

The number of terms may be greater reduced due to some special symmetries of  $C_{ijkl}$ . The Voigt's convention is used to denote each pair of indexes of the elastic constants defined by (3) by a single index

$$C_{1111} \rightarrow C_{11}, C_{1122} \rightarrow C_{12}, C_{1133} \rightarrow C_{13}, C_{3333} \rightarrow C_{33}, C_{2323} \rightarrow C_{44}, C_{1212} \rightarrow C_{66}.$$

The independent non-zero elastic constants after the biaxial deformation are then given by

$$C_{11} = A_{11} - B_{11}, \quad C_{22} = C_{33} = A_{22} - B_{22}, \quad C_{44} = 1/2(C_{22} - C_{23}), \\ C_{55} = C_{66} = A_{13} - B_{55},$$

$$C_{12} = C_{13} = A_{13}, \quad C_{23} = (1/3)A_{22}, \quad C_{25} = C_{46} = A_{25}, \quad C_{35} = A_{25} \quad A_{11} = (2/3)f_c \eta'^4, \\ A_{22} = (1/16)(9f_a + f_c)\eta^4, \quad A_{13} = (1/6)f_c \eta^2 \eta'^2, \quad A_{25} = (1/12\sqrt{2})f_c \eta^3 \eta', \\ B_{11} = 8g_c \eta'^2, \quad B_{22} = (6g_a + 2g_c)\eta^2, \quad B_{55} = 0.5[3g_a \eta^2 + g_c(\eta^2 + 4\eta'^2)], \\ f_a = f(R_a), \quad f_c = f(R_c), \quad g_a = g(R_a), \quad g_c = g(R_c), \quad R_a = (1/\sqrt{2})\eta a, \\ R_c = a\sqrt{(1/3)\eta'^2 + (1/6)\eta^2}, \quad \eta = 1 + \varepsilon, \quad \eta' = 1 + \varepsilon'.$$

The biaxial modulus is defined as the stress-strain ratio  $Y_b = \sigma/\varepsilon$ , where assuming symmetry in the  $X_2, X_3$  plane yields. The  $Y_b$  can be measured with a bulge test in a thin structure: it represents the stress over strain ratio for stretching without shear ( $\sigma_4 = 0$ ). The condition  $\sigma_1 = \sigma_5 = \sigma_6 = 0$  gives the natural boundary conditions, since there cannot be any stress component outside the  $X_2, X_3$  plane. Due to the assumed symmetry in the  $X_2, X_3$  plane, it follows

$$\varepsilon_2 = \varepsilon_3 = (S_{22} + S_{23})\sigma, \quad Y_b = 1/(S_{22} + S_{23}), \quad (10)$$

where  $S_{ij}$  is the elastic compliance tensor, which is the inverse of the stiffness tensor  $S_{ij}C_{jk} = \delta_{ik}$ . For special symmetries, e.g. trigonal in our case, it is possible to find simple relationships between the components of the stiffness and compliance tensors

$$\varepsilon' = \varepsilon_1 = -2\varepsilon C_{12}/C_{11}, \quad Y_b = C_{22} + C_{23} - 2C_{12}^2/C_{11}. \quad (11)$$

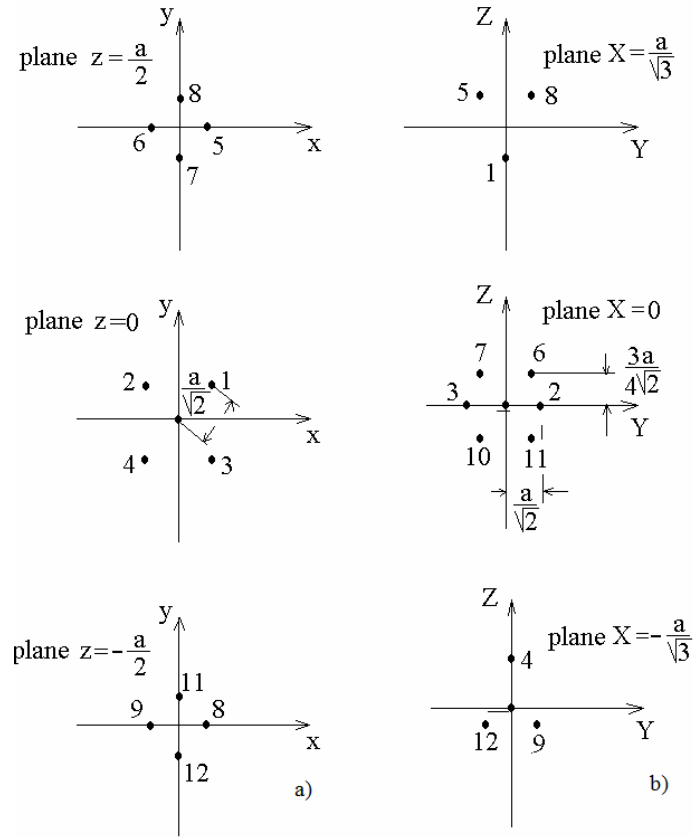


Fig. 5 – Representation of the twelve nearest neighbours:  
a) in  $(x, y, z)$  system; b) in  $(X, Y, Z)$  system.

### 3. COMPOSITES WITH NEGATIVE STIFFNESS INCLUSIONS

Let us assume that an BC crystal cell is biaxial deformed in the  $[111]$  direction. The theory of small, infinitesimal elastic deformations superimposed on a finite elastic deformation is used to analyze the effect of the initial deformations upon the elastic constants. The negative stiffness mechanism and incorporating into the matrix are defined in terms of the Eshelby's steps [15]: 1) a FCC crystal cell belonging to the cubic system is subjected to a stress-free biaxial deformation in the  $[111]$  direction, becoming trigonal; 2) apply a surface biaxial traction to the trigonal crystal to be incorporated into the polymeric matrix, by assuring the continuity of displacements and normal stresses across the boundaries.

The initial underformed BC is a cubic one. We used here the Voigt's convention to denote each pair of indexes of the elastic constants by a single index



$$\begin{aligned} C_{1111} &\rightarrow C_{11}, & C_{1122} &\rightarrow C_{12}, & C_{1133} &\rightarrow C_{13}, \\ C_{3333} &\rightarrow C_{33}, & C_{2323} &\rightarrow C_{44}, & C_{1212} &\rightarrow C_{66}. \end{aligned} \quad (12)$$

To study the crystal in a biaxial deformed state, the three configurations with the same origin O are:

- the natural or stress-free configuration  $C_0$ ;
- the initially deformed equilibrium configuration  $\tilde{C}$ ;
- the present configuration  $C(t)$ .

The geometrical system  $(x') = O x'_1 x'_2 x'_3$  exploits the geometric symmetry of the body or the symmetry of the stress state. The axis  $x'_3$  is parallel to the texture direction, i.e. the modulation or the growth direction [111]. The orientation of the axes  $x'_1, x'_2$  (usually randomly oriented in the plane of the foil perpendicularly on the texture direction) is determined by the angle  $\psi$ . The transformation from  $(\xi)$  to  $(x')$  is given by  $x'_i = R_{ik} \xi_k$ , where  $R_{ij}$  is the rotation matrix.

By carrying the crystal from  $C_0$  to  $\tilde{C}$ , the crystal has the constants

$$\begin{aligned} C'_{11} &= \alpha_{11} = (c_{11}^0 + c_{12}^0 + 2c_{44}^0)/2, \\ C'_{22} &= \alpha_{22} = (c_{11}^0 + 2c_{12}^0 - c_{44}^0)/6, \\ C'_{44} &= \alpha_{44} = (c_{11}^0 + 2c_{12}^0 + 4c_{44}^0)/3, \\ C'_{12} &= \alpha_{12} = \alpha_{21} = (c_{11}^0 + 5c_{12}^0 - 2c_{44}^0), \\ C'_{23} &= \alpha_{23} = \alpha_{32} = (c_{11}^0 + 2c_{12}^0 - 2c_{44}^0)/3, \\ C'_{44} &= \alpha_{44} = (c_{11}^0 - c_{12}^0 + c_{44}^0)/3, \\ C'_{55} &= \alpha_{55} = (c_{11}^0 - c_{12}^0 + c_{44}^0)/6, \\ C'_{25} &= \alpha_{25} = \alpha_{52} = (c_{11}^0 + c_{12}^0 - 2c_{44}^0)/6. \end{aligned} \quad (13)$$

The relation between  $C'_{ijkl}$  and  $\tilde{C}_{ijkl}$  are given by

$$\tilde{C}_{ijkl} = \left( \frac{\mathbf{X}}{\xi} \right)^{-1} \frac{\partial X_i}{\partial \xi_\mu} \frac{\partial X_j}{\partial \xi_\nu} \frac{\partial X_k}{\partial \xi_\nu} \frac{\partial X_l}{\partial \xi_\nu} C'_{\mu\rho\nu\varsigma}. \quad (14)$$

We obtain

$$r_P = r_Q + n_1 d_1 + n_2 d_2. \quad (15)$$

$$\begin{aligned}
\tilde{C}_{11} &= \frac{(1+\varepsilon)^2}{36(1+\varepsilon_3)} C'_{11}, & \tilde{C}_{22} &= \frac{1}{6} \left( -\frac{(1+\varepsilon)^2}{2(1+\varepsilon_3)} + \frac{1}{3}(1+\varepsilon_3) \right) C'_{22}, \\
\tilde{C}_{12} &= \frac{(1+\varepsilon)^2}{12(1+\varepsilon_3)} C'_{12}, & \tilde{C}_{23} &= \frac{1}{6}(1+\varepsilon_3) C'_{12}, & \tilde{C}_{25} &= \frac{(1+\varepsilon_3)^3}{9(1+\varepsilon)^2} C'_{33}, \\
\tilde{C}_{44} &= \frac{1}{6} \left( -\frac{1}{2} \frac{(1+\varepsilon)^3}{(1+\varepsilon_3)^2} + \frac{1}{3}(1+\varepsilon_3) \right) C'_{44}, & \tilde{C}_{55} &= \frac{1}{4} \left( -\frac{(1+\varepsilon_3)^2}{3(1+\varepsilon)} + \frac{1}{2}(1+\varepsilon) \right) C'_{66}, \\
\tilde{C}_{35} &= \left( \frac{(1+\varepsilon_3)^3}{7(1+\varepsilon)^2} + \frac{1}{9}(1+\varepsilon) \right) C'_{33},
\end{aligned} \tag{15}$$

where  $\varepsilon_i$  are the biaxial deformations in the Voigt's notation

$$\begin{aligned}
\varepsilon_{11} &= \varepsilon_1, & \varepsilon_{22} &= \varepsilon_2, & \varepsilon_{33} &= \varepsilon_3, & 2\varepsilon_{23} &= \varepsilon_4, \\
2\varepsilon_{13} &= \varepsilon_5, & 2\varepsilon_{12} &= \varepsilon_6, \\
\varepsilon_1 &= \varepsilon_2 = \varepsilon, & \varepsilon_3 &= -2 \frac{C'_{13}}{C'_{33}} \varepsilon, & \varepsilon_4 &= \varepsilon_5 = \varepsilon_6 = 0.
\end{aligned} \tag{16}$$

Assuming symmetry in the  $X_2 - X_3$  plane the biaxial stresses are (stretching without shear)

$$\sigma_1 = \sigma_2 = \sigma, \quad \sigma_3 = \sigma_4 = \sigma_5 = \sigma_6 = 0. \tag{17}$$

We compute all elastic constants by using (8) and (9). There are two parameters in our formulae that need to be specified:  $\alpha$  (units Ryd (Rydberg), 1 Ryd = 13.6 eV =  $2.092 \times 10^{-21}$  J) and  $\beta$  (units ua in units of  $a^{-1}$ , where  $a$  is the lattice constant). The chosen of  $\alpha$  is irrelevant since it affects only the absolute values of the elastic constants and moduli as a multiplicative constant whereas we are interested in their relative change. To give it value, we need it as a free parameter to fit the experimental value of  $C_{11}$  in the case of zero deformation in  $(x, y, z)$  reference system. For Cu it is obtained  $\alpha = 0.3415 \times 10^6$  Ryd, and for Au and Ag  $\alpha = 0.36 \times 10^6$  Ryd [14]. From the same source we have  $\beta = 13.84$  ua for Cu,  $\beta = 12$  ua for Au and  $\beta = 12.24$  ua for Ag.

The properties of resin are: the Young's modulus 0.5 GPa, the Poisson's ratio 0.49 and density 980 kg/m<sup>3</sup>. The initially properties of the BC crystal cell are: the Young's modulus 197 GPa, the Poisson's ratio 0.3 and density 7 850 kg/m<sup>3</sup>.

After biaxial deformation of the BC crystal cell, all independent elastic constants and the corresponding biaxial modulus and shear modulus are evaluated for strains between  $-10\%$  and  $10\%$ .

The modulus  $Y_b$  can be measured with a bulge test in a thin film: it represents the stress over strain ratio for a stretching of the film without shear ( $\sigma_4 = 0$ ). The equations  $\sigma_1 = \sigma_5 = \sigma_6 = 0$  give the natural boundary conditions, since there cannot be any stress component outside the  $X_2 - X_3$  plane. Due to the assumed symmetry in the  $X_2 - X_3$  plane

$$\varepsilon_2 = \varepsilon_3 = (S_{22} + S_{23})\sigma, \quad (18)$$

and

$$Y_b = \frac{1}{S_{22} + S_{23}}. \quad (19)$$

In (18) and (19)  $S_{ij}$  is the elastic compliance tensor, which is the inverse of the stiffness tensor

$$S_{ij}C_{jk} = \delta_{ik}. \quad (20)$$

For special symmetries, e.g. trigonal in our case, it is possible to find simple relationships between the components of the stiffness and compliance tensors. We obtain

$$\varepsilon' = \varepsilon_1 = -2\frac{C_{12}}{C_{11}}\varepsilon, \quad Y_b = C_{22} + C_{23} - 2\frac{C_{12}^2}{C_{11}}. \quad (21)$$

We have evaluated all the independent elastic constants and the corresponding biaxial modulus  $Y_b$  for strains between  $-10\%$  and  $10\%$ , the numerical results are plotted in Figs.6 and 7. The reported values refer to the system of axes  $(X, Y, Z)$ .

Figures 6 and 7 show that a relatively small deformation may lead to a large change in  $Y_b$  due mainly to the contribution of  $C_{22}$ . The biaxial modulus become negative for relative large deformations (0.081, 0.1).

For strain in the range (0.01, 0.0845) this constant becomes negative. The constant  $C_{44}$  is negative in the same range of strains. The constants  $C_{11}$  is negative for (0.024, 0.845). The constants  $C_{11}, C_{44}$  and  $C_{55}$  become negative in the range  $(-0.06, -0.0844)$ . The constant  $C_{55}$  is negative for (0.04, 0.0845), the constant  $C_{12}$  for (0.06, 0.092) and  $C_{23}$  for (0.06, 0.0845).

The common interval for all constants to be negative is (0.06, 0.845).

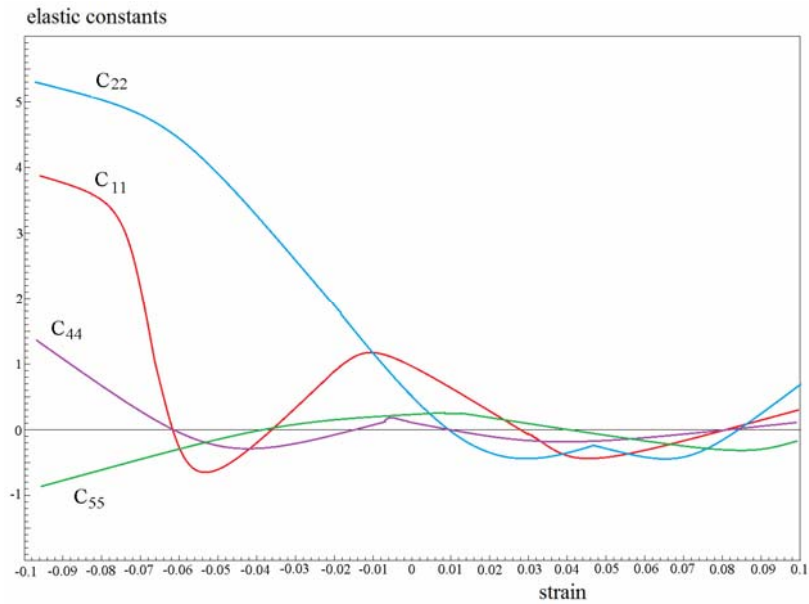


Fig. 6 – Plots of the elastic constants in the  $(X, Y, Z)$  system as a function of the strain. The units are  $10^3 \text{ GPa}$ .

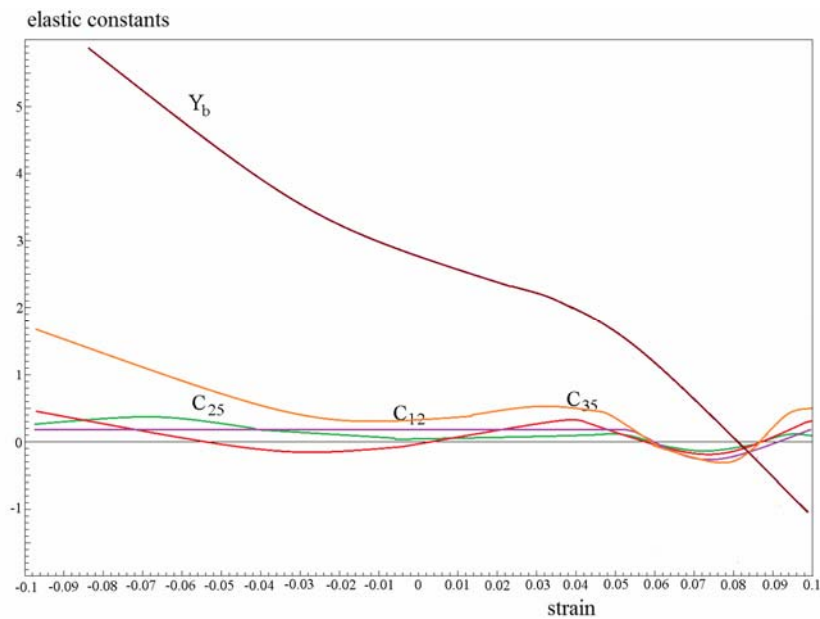


Fig. 7 – Plots of the elastic constants in the  $(X, Y, Z)$  system as a function of the strain. The units are  $10^3 \text{ GPa}$ .

The variation of force with respect to displacement in the composite is shown in Fig. 8, where the negative stiffness effect contribution to the total force is exhibited.

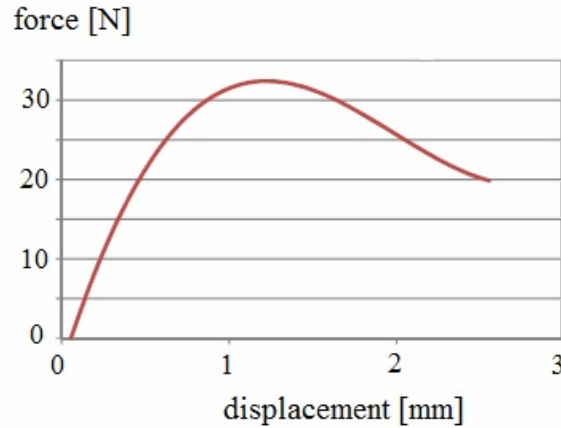


Fig. 8 –Variation of force with respect to displacement in the composite.

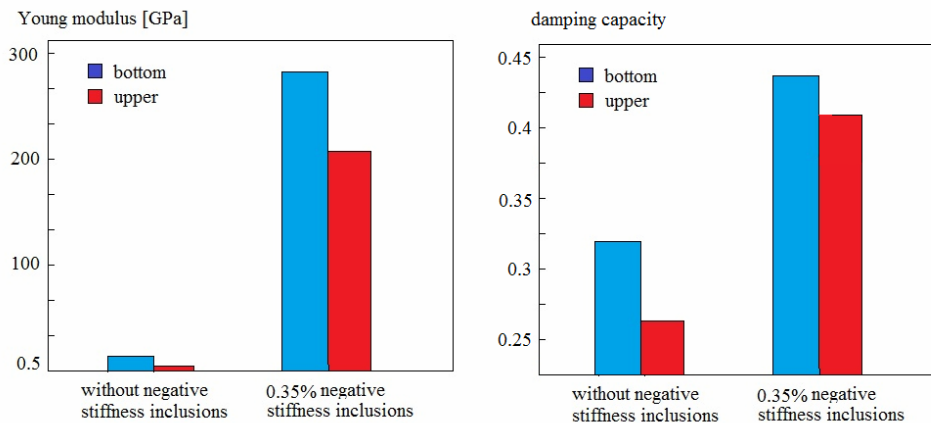


Fig. 9 – Young elastic modulus and damping capacity, for the resin matrix without the negative stiffness inclusions, and for composite with the negative stiffness inclusions, respectively.

In Fig. 9 we can see the results of Young elastic modulus and damping capacity, for the resin matrix without the negative stiffness inclusions, and for composite with the negative stiffness inclusions, respectively. The Young modulus increases for addition of negative stiffness inclusions. The damping capacity also increases for addition of negative stiffness inclusions due to the high energy absorbance of inclusions. As a general observation, for both elastic modulus and damping capacity, their increasing is a result of negative elastic constants of the inclusions.

#### 4. CONCLUSIONS

A composite consisted by the negative stiffness inclusion encapsulated by a polymer matrix is considered in this paper. The property of negative stiffness is usually unstable, but the inclusions of negative stiffness can be stabilized within a positive-stiffness material.

The negative stiffness mechanism and incorporating into the matrix are defined in terms of the Eshelby's steps: 1) a FCC crystal cell belonging to the cubic system is subjected to a stress-free biaxial deformation in the [111] direction, becoming trigonal; 2) apply a surface biaxial traction to the trigonal crystal to be incorporated into the polymeric matrix, by assuring the continuity of displacements and normal stresses across the boundaries.

As a consequence, the negative stiffness inclusion becomes a trigonal structure with 8 elastic constants  $\tilde{C} = \{\tilde{C}_{11}, \tilde{C}_{22}, \tilde{C}_{44}, \tilde{C}_{55}, \tilde{C}_{12}, \tilde{C}_{23}, \tilde{C}_{25}, \tilde{C}_{35}\}$  given by (15). All the independent elastic constants and the corresponding biaxial modulus  $Y_b$  for strains between  $-10\%$  and  $10\%$  are evaluated. The common strain interval for all constants to be negative is  $(0.06, 0.845)$ . A relatively small deformation may lead to a large change in  $Y_b$  due mainly to the contribution of  $C_{22}$ . The biaxial modulus become negative for relative large deformations  $(0.081, 0.1)$ . Finally, we show that, by embedding of negative stiffness inclusions within a polymeric matrix, the stiffness of the polymer increases, and also, a superior damping capacity is obtained. The negative stiffness inclusions are excellent mechanisms for use in vibrational and acoustic damping

**Acknowledgements.** The authors gratefully acknowledge the financial support of the National Authority for Scientific Research ANCS/UEFISCDI through the project PN-II-ID-PCE-2012-4-0023, Contract no. 3/2013.

*Received on June 12, 2016*

#### REFERENCES

1. CHRONOPOULOS, D., ANTONIADIS, I., COLLET, M., ICHCHOU, M., *Enhancement of wave damping within metamaterials having embedded negative stiffness inclusions*, Wave Motion, **58**, pp. 165–179, 2015.
2. CHRONOPOULOS, D., ANTONIADIS, I., AMPATZIDIS, T., *Enhanced acoustic insulation properties of composite metamaterials having embedded negative stiffness inclusions*, Extreme Mechanics Letters, **12**, pp. 48-54, 2017.
3. RODRIQUEZ, N. COBO-LOSEY, *Design and testing of negative stiffness inclusions for damping materials*, PhD thesis, Escuela Técnica Superior de Ingeniería (ICAI), Universidad Pontificia Comillas, Madrid, Spain, 2016.

4. LAKES, R.S., *Extreme damping in composite materials with a negative stiffness phase*, Phys. Rev. Lett., **86**, 13, pp. 2897-2900, 2001.
5. LAKES, R.S., LEE, T., BERSIE, A., WANG, Y.C., *Extreme damping in composite materials with negative stiffness inclusions*, Nature, **410**, 565–567, 2001.
6. LAKES, R. S., DRUGAN, W.J., *Dramatically stiffer elastic composite materials due to a negative stiffness phase*, J. of the Mechanics and Physics of Solids, **50**, 5, pp. 979–1009, 2002.
7. CHIROIU, V., MUNTEANU, L., DUMITRIU, D., BELDIMAN, M., SECARA, C., *On the architecture of a new cellular elastic material*, Proceedings of the Romanian Academy, Series A: Mathematics, Physics, Technical Sciences, Information Science, **9**, 2, pp. 105–115, 2008.
8. CHIROIU, V., MUNTEANU, L., DUMITRIU, D., *The relationship between the behavior of auxetic and negative stiffness materials. Part I: Theory*, The International Review of Mechanical Engineering (IREME), **2**, 1, pp. 73–85, 2008.
9. SANDLER, S., WRIGHT, J.P., In: *Theoretical foundation for large scale computations of nonlinear material behavior*, Eds. S. Nemat Nasser, R.J. Asaro, G.A. Hegemier, M. Nijhoff, 1984.
10. TEODORESCU, P.P., MUNTEANU, L., CHIROIU, V., *On the wave propagation in a chiral Cosserat medium*, in: *New Trends in Continuum Mechanics, Theta Series in Advanced Mathematics*, Ed. Theta Foundation, Bucharest, 2005, pp. 303–310.
11. TEODORESCU, P.P., BADEA, T., MUNTEANU, L., ONISORU, J., *On the wave propagation in composite materials with a negative stiffness phase*, in: *New Trends in Continuum Mechanics, Theta Series in Advanced Mathematics*, Edit. Theta Foundation, Bucharest, 2005, pp. 295–302.
12. JANKOWSKI, A.F., TSAKALAKOS, T., *The effect of strain on the elastic constants of noble metals*, J. Phys. F: Met. Phys., **15**, 6, pp. 1279–1292, 1985.
13. JANKOWSKI, A.F., *Modelling the supermodulus effect in metallic multilayers*, J. Phys. F: Met. Phys., **18**, 3, pp. 413–427, 1988.
14. DELSANTO, P.P., PROVENZANO, V., UBERALL, H., *Coherency strain effects in metallic bilayers*, J. Phys.: Condens. Matter., **4**, 15, pp. 3915–3928, 1992.
15. ESHELBY, J.D., *The determination of the elastic field of an ellipsoidal inclusion and related problem*, Proc. R. Soc. A, **241**, pp. 376–396, 1957.